Neuron 52, 425–436, November 9, 2006 ©2006 Elsevier Inc. DOI 10.1016/j.neuron.2006.08.028

Refined Spatial Manipulation of Neuronal Function by Combinatorial Restriction of Transgene Expression

Neurotechnique

Haojiang Luan,[1] Nathan C. Peabody,[1] Charles R. Vinson,[2] and Benjamin H. White[1,*]

[1] Laboratory of Molecular Biology
National Institute of Mental Health
[2] Laboratory of Metabolism
National Cancer Institute
National Institutes of Health
9000 Rockville Pike
Bethesda, Maryland 20892

Summary

Selective genetic manipulation of neuronal function in vivo requires techniques for targeting gene expression to specific cells. Existing systems accomplish this using the promoters of endogenous genes to drive expression of transgenes directly in cells of interest or, in "binary" systems, to drive expression of a transcription factor or recombinase that subsequently activates the expression of other transgenes. All such techniques are constrained by the limited specificity of the available promoters. We introduce here a combinatorial system in which the DNA-binding (DBD) and transcription-activation (AD) domains of a transcription factor are independently targeted using two different promoters. The domains heterodimerize to become transcriptionally competent and thus drive transgene expression only at the intersection of the expression patterns of the two promoters. We use this system to dissect a neuronal network in *Drosophila* by selectively targeting expression of the cell death gene *reaper* to subsets of neurons within the network.

Introduction

Understanding how individual neurons, or subsets of neurons, contribute to the development and function of neuronal networks requires techniques for selectively manipulating their function. A growing number of methods exists for perturbing neuronal function by expressing transgenes that affect signaling pathways or cellular viability (reviewed in Miesenbock and Kevrekidis, 2005; White et al., 2001; Wulff and Wisden, 2005), but methods for selectively deploying the expression of these transgenes to specific subsets of neurons remain limited. Binary techniques have proven extremely useful in expressing foreign transgenes in patterns dictated by the promoters of individual endogenous genes (for review see Mallo, 2006), but because most genes are expressed broadly and dynamically, these patterns are rarely restricted enough to map the functional identities of cells within specific developmental lineages or neuronal networks.

To provide further restriction of transgene expression, several ternary techniques have been introduced that place binary gene activation under the control of a third component. In *Drosophila*, the Gal4-UAS system (reviewed in Duffy, 2002), which uses the yeast transcription factor Gal4 to activate expression of transgenes placed downstream of its unique "upstream activating sequence," or UAS, has been augmented by the addition of the Gal4 repressor, Gal80. Targeting of Gal80 expression to subsets of cells can then be used to restrict gene expression (Suster et al., 2004), in some cases with single-cell resolution, as in the widely used MARCM system (Lee and Luo, 1999). Alternatively, a "Flp-in" technique, which makes UAS-transgene activation contingent on excision of an inserted "stop cassette" by the Flp-recombinase, has been used to restrict expression by independently targeting Gal4 and Flp using different promoters (Stockinger et al., 2005). Similarly in mice, transgene activation has been made contingent on the activity of two independently targeted recombinases by coupling Flp to the Cre-lox system, as in the "intersectional gene activation" technique (Awatramani et al., 2003; Farago et al., 2006).

To date, ternary systems have been developed primarily for use in developmental studies to restrict reporter transgene expression to small numbers of neurons for lineage analysis and fate mapping. Most can, in principle, also be used to drive effector transgene expression to manipulate neuronal function, but usually with certain limitations. Restriction using the MARCM technique, for example, is limited to clonally derived neurons and constrained by the developmental timing of mitosis in the lineages under study. In recombinase-based systems, inefficiency of recombination can limit the extent of gene activation (Ting et al., 2005). Such systems are also intrinsically irreversible.

To develop an alternative ternary approach for versatile functional manipulation of neuronal activity, we have taken advantage of the modularity of transcription factors, which, as first shown for the yeast transcriptional activator Gal4 (Brent and Ptashne, 1985; Keegan et al., 1986), often consist of separable functional domains for site-specific DNA binding (DBD) and transcription activation (AD). Neither domain can activate transcription on its own, but when joined, either covalently or by noncovalent interactions, the two domains can reconstitute site-specific gene expression at appropriate promoter sites. This modularity has been exploited previously in the construction of chimeric transcription factors (Gossen and Bujard, 1992; Wang et al., 1994) and in transcription-based assays for protein interaction domains, such as the widely used yeast two-hybrid system (Fields and Song, 1989). In the "Split Gal4" system described here, we have also exploited this modularity to design DBD and AD domains, which can be independently targeted using different promoters. Each domain is fused to a heterodimerizing leucine zipper fragment so that the two domains bind tightly when expressed together in the same cell to become transcriptionally active. By anchoring the expression of one domain to the expression pattern of one promoter and using other promoters to drive expression of the other domain, transcriptional activity can be reconstituted within restricted

*Correspondence: benjaminwhite@mail.nih.gov

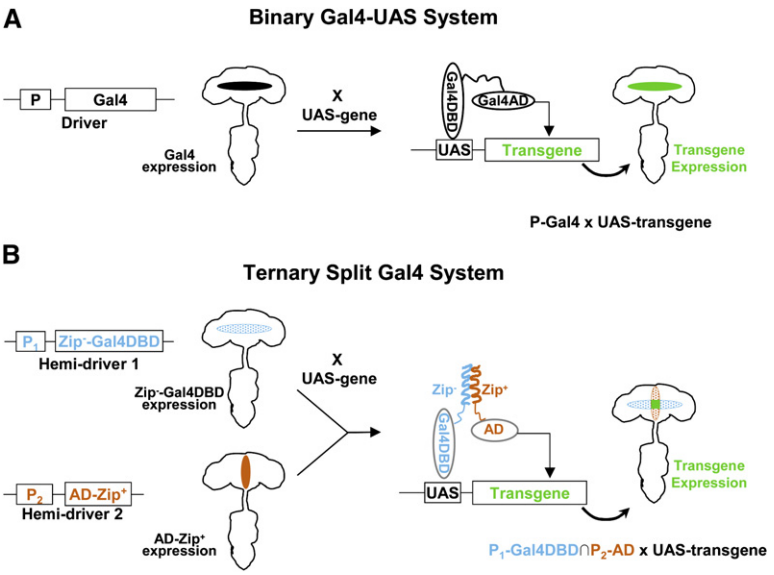

Figure 1. The Ternary Split Gal4 System Improves upon Existing Binary Expression Systems in Restricting Transgene Expression

(A) Schematic depiction of the Gal4-UAS system of *Drosophila,* a classic binary system for targeting transgene expression in vivo. The first essential component of this system, shown at left, is a transgene containing the yeast transcription factor Gal4 downstream of a promoter/enhancer (P). P drives expression of Gal4 in flies bearing this transgene in a cell type-specific manner (shown as a black region within the CNS). When flies bearing Gal4 are crossed to flies bearing the second component of the system, a transgene of interest placed downstream of the Gal4 DNA recognition site or UAS, this transgene is also expressed in the same cell type-specific manner (right).

(B) The Split Gal4 system exploits the fact that the two functional domains of Gal4, the DNA-binding (DBD) and transcription-activation (AD) domains, are separable. In the Split Gal4 system each domain is fused to a heterodimerizing leucine zipper (Zip^+ or Zip^-) to insure that the two domains associate when expressed in the same cell and reconstitute transcriptional activity. Starting at left, the schematic shows that the Gal4DBD and AD constructs can be independently targeted using different promoters/enhancers (P_1 and P_2). When these constructs ("hemidrivers") are brought together in crosses to flies bearing a UAS-transgene, the transgene is expressed in progeny only at the intersection of the expression patterns of P_1 and P_2 (designated by the intersection sign, ∩), where transcriptional activity is reconstituted, as shown on the bottom right. The Gal4DBD must be used if UAS-transgenes are to be transcribed, but any transcription-activation domain can be used, as long as it is fused to the leucine zipper fragment complementary to that fused to Gal4DBD.

regions of the initial pattern. We introduce two implementations of this method in which the DBD of the yeast transcription factor Gal4 is used in conjunction with either the Gal4 AD or the activation domain of the more potent viral transcription factor, VP16. We demonstrate the utility of the system by functionally dissecting a simple neural network involved in wing expansion in *Drosophila*. We anticipate that the Split Gal4 system will be broadly applicable to problems in which manipulation of cellular function must be rationally restricted.

Results and Discussion

Development of the Split Gal4 System

To implement the strategy of restricting transgene expression in vivo by independently targeting transcription factor domains, we developed tools that could be deployed in the fruit fly, *Drosophila melanogaster*, in which the binary Gal4-UAS system for transgene expression is already well established (Figure 1A, Brand and Perrimon, 1993). This system includes several hundred transgenic fly lines designed to express reporter and effector transgenes under the control of the "upstream activating sequence" recognized by the Gal4 DBD. We therefore sought to develop a system (Figure 1B) in which the Gal4 DBD was paired with an AD potent enough to drive transgene expression at levels high enough to permit manipulation of cellular function. Previous studies have indicated that the primary Gal4 AD (i.e., "region II," Ma and Ptashne, 1987b) coupled with the Gal4 DBD might promote transcription at levels that are only a fraction of those produced by intact Gal4 (Ma and Ptashne, 1987a). We therefore also tested the more potent AD from the Herpes Simplex Virus 1 transcription factor, VP16.

To optimize transcriptional activity, we fused the Gal4 DBD and the ADs to heterodimerizing leucine zippers, varying the zipper type, site of fusion (N or C terminus), and length of the polyglycine spacer between the zipper and the transcription factor domains (see Table S1 in the Supplemental Data for details). The constructs that produced maximal transcriptional activity when cotransfected into *Drosophila* SL-2 cells are shown schematically in Figure 2A. These optimal constructs incorporated synthetic leucine zippers based on the chicken B-Zip family member Vitellogenin Binding Protein (Moll et al., 2001). The sequences of these zippers do not match those of *Drosophila* B-Zip family members (Fassler et al., 2002) and were selected for their strong heterodimerizing and low homodimerizing potentials. Transcriptional activities of the optimal constructs, expressed pairwise in transfected cells and measured in terms of the relative enzymatic activity of a UAS-β-galactosidase reporter, were 52% and 84% of that of intact Gal4 for the Gal4DBD-Gal4AD and the Gal4DBD-VP16AD pairs, respectively (Figure 2B). The individual optimized constructs, which we refer to as "hemidrivers," displayed little to no transcriptional activity when transfected alone.

In Vivo Characterization of the Split Gal4 System

We evaluated the efficacy of the optimized hemidrivers in vivo in three steps, increasing restriction of transgene expression at each step. In step 1, we created and crossed transgenic lines that expressed each hemidriver throughout the nervous system. This permitted evaluation of each hemidriver's ability to promote neuronal transgene expression when used in concert with complementary hemidrivers. In addition, it permitted the assessment of possible side effects of each

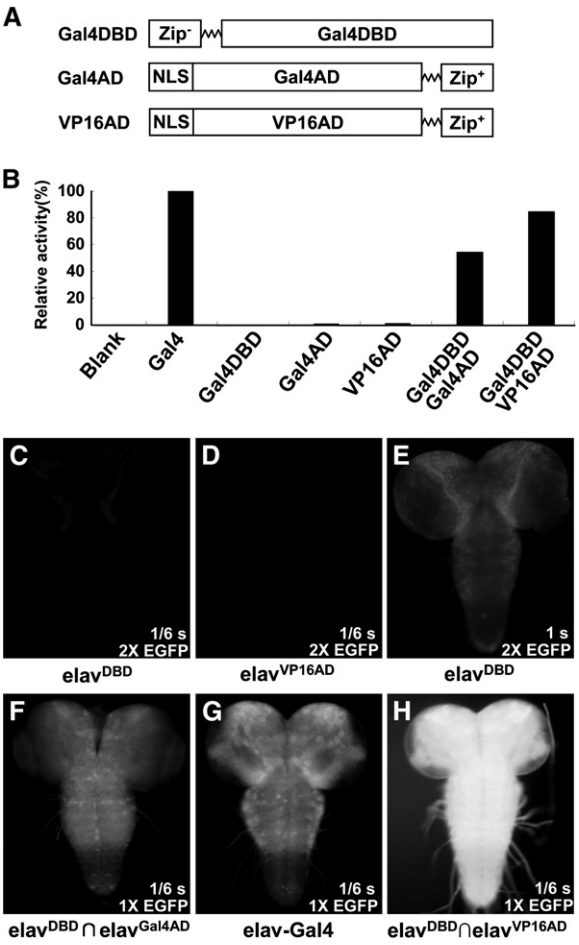

Figure 2. Optimized Split Gal4 Constructs Efficiently Drive UAS-Reporter Gene Expression In Vitro and In Vivo in the *Drosophila* Nervous System

(A) Schematic representation of the three optimized Split Gal4 constructs: (top) the DNA-binding domain of the Gal4 molecule fused at the N terminus to the Zip^- leucine zipper (see Experimental Procedures), (middle) the major transcription-activation domain of Gal4 fused at the C terminus to the Zip^+ leucine zipper (Gal4AD), and (bottom) a similar AD construct containing the C-terminal acidic domain of the VP16 transcription factor. The sawtooth line represents a flexible linker of ten consecutive glycine residues. NLS, SV40 nuclear localization signal. The Gal4DBD contains an endogenous N-terminal NLS (not depicted).

(B) Relative transcriptional activities of the Split Gal4 constructs when expressed in cultured cells, alone and in combination. Transcriptional activity was measured indirectly as the β-galactosidase activity in lysates of *Drosophila* SL-2 cells cotransfected with plasmids containing the indicated Split Gal4 constructs and a UAS-LacZ gene. β-galactosidase activity was normalized to the total protein and is expressed as the percentage of the activity measured in cells transfected with intact Gal4. Bars show average activity in three transfections.

(C–H) Fluorescence photomicrographs of *Drosophila* third-instar larval CNS from animals expressing (C) Gal4DBD alone, (D) VP16AD alone, (E) Gal4DBD alone, (F) Gal4DBD and Gal4AD, (G) intact Gal4, or (H) Gal4DBD and VP16AD. Expression was driven by the panneuronal elav promoter. Fluorescence shows expression of one or two copies of a UAS-EGFP reporter transgene, as indicated. (E) Long-exposure image (6-fold longer than for the other panels) reveals weak expression of the reporter driven by the Gal4DBD construct alone. Here and elsewhere, hemidrivers are denoted by the promoter used to drive the (superscripted) Split Gal4 construct, with Gal4DBD abbreviated to DBD, and ∩ denotes the combination of hemidrivers expressed in a cross.

hemidriver's individual expression. In step 2, we created lines that expressed each hemidriver in a small set of identified neurons that expresses Crustacean Cardioactive Peptide (CCAP). Crosses of these lines to complementary, panneuronal hemidriver lines from step 1 permitted rigorous evaluation of each hemidriver's ability to faithfully restrict transgene expression to a set of neurons. In step 3, we created lines that overlapped in expression pattern with the lines created in step 2, but only within distinct subsets of the CCAP-expressing neurons. This permitted validation of the Split Gal4 system as a tool for mapping the functional identities of defined subsets of neurons. The results obtained at each step of evaluation are discussed in the sections below, with the headings indicating whether the promoters used to express the hemidrivers (P_1 and P_2) drive transgene expression in a common set of neurons (P_1 equals P_2), in an included subset (P_1 includes P_2), or in the intersection of two distinct sets (P_1 overlaps P_2).

Step 1: Panneuronal Expression Using the Split Gal4 System (P_1 Equals P_2)

Transgenic fly lines that expressed each hemidriver panneuronally were made using the promoter of the *elav* gene (Yao and White, 1994) and are referred to as $elav^{Gal4DBD}$, $elav^{Gal4AD}$, and $elav^{VP16AD}$. These lines were viable and healthy, suggesting that expression of the transcription factor constructs throughout the nervous system is not deleterious in itself. In addition, the individual hemidrivers appeared transcriptionally inactive in vivo, just as they were in vitro. The progeny of crosses of each hemidriver line to a line carrying a UAS-EGFP or UAS-EYFP reporter transgene did not exhibit obvious nervous system fluorescence at any stage of development (data not shown). This was true even for homozygous animals containing two copies each of the single hemidrivers and the UAS-EGFP transgenes (Figures 2C and 2D), although at long exposure times limited fluorescence was observed in animals expressing two copies of $elav^{Gal4DBD}$ (Figure 2E), suggesting that this hemidriver may have weak transcriptional activity on its own.

In contrast, pairwise crosses of $elav^{Gal4DBD}$ and $elav^{Gal4AD}$ lines in the presence of a UAS-reporter yielded progeny with bright fluorescence specifically expressed in the central nervous system (CNS; Figure 2F). We designate crosses in which DBD and AD hemidrivers are paired, with the intersection symbol, ∩. All $elav^{Gal4DBD}$ ∩ $elav^{Gal4AD}$ crosses, yielded viable progeny that expressed the reporter transgenes in the nervous system, in some cases at levels approaching that of intact Gal4 (Figure 2G). Nervous system fluorescence was strong enough to be observed by epifluorescence under a dissection microscope as well as by confocal microscopy from the late embryonic period through adulthood.

Crosses in which the $elav^{Gal4DBD}$ and $elav^{VP16AD}$ hemidrivers were paired yielded viable adult progeny with even stronger nervous system fluorescence (Figure 2H), though, as noted in Experimental Procedures, many of these crosses were lethal. Lethality was independent of reporter gene expression and has not been observed in any other crosses, including those that drive expression in all cholinergic neurons, which comprise much

of the fly nervous system, or in broad patterns defined by VP16AD enhancer-trap lines (see below). Overall, our observations strongly indicate that toxicity is not a general feature of VP16AD and Gal4DBD coexpression in neurons and may instead result from disruption of function in a small number of cells variably represented in the expression pattern of the elav promoter.

Step 2: The Split Gal4 System Can Faithfully Target Gene Expression to a Subset of Neurons (P_1 Includes P_2)

To confirm the ability of the Split Gal4 system to restrict transgene expression to a subset of cells within the pattern dictated by a promoter of interest, we first sought to limit UAS-EGFP expression within the nervous system to an identified set of neurons. To this end, we generated a second set of hemidrivers ($CCAP^{Gal4DBD}$, $CCAP^{Gal4AD}$, and $CCAP^{VP16AD}$) using the promoter for the CCAP gene, which has been demonstrated previously (Park et al., 2003) to be active in approximately 50 neurons of the larval central nervous system (Figures 3A and 3B). We then performed pairwise crosses, combining complementary transcription factor domains expressed under the control of the elav and CCAP promoters, and monitored the pattern of expression of a UAS-EGFP reporter transgene in the progeny.

The $elav^{Gal4DBD} \cap CCAP^{Gal4AD}$ crosses resulted in UAS-EGFP expression exclusively within the more restricted CCAP pattern (Figure 3C), consistent with the reconstitution of transcriptional activity in only cells expressing both transcription factor domains. The reciprocal crosses, namely $CCAP^{Gal4DBD} \cap elav^{GAL4AD}$, gave similar results (data not shown), and in both cases expression within the CCAP-expressing neurons (N_{CCAP}) was confirmed by double labeling with an anti-CCAP antibody (Figures S1A–S1C). In most crosses, some expression was seen in small numbers of non-CCAP-immunoreactive neurons. This lack of fidelity was similar in exent to that observed with the CCAP-Gal4 driver line created by Park et al. (2003), the expression pattern of which includes non-CCAP-expressing neurons in some animals (see legend, Figure 3B). With both Gal4 drivers and Split Gal4 hemidrivers, "position effects" resulting from the action of genomic enhancers adjacent to the site(s) of transgene insertion are thus likely to perturb the transcriptional activity of the CCAP-promoter.

We determined the frequency of reporter gene expression in individual CCAP-immunopositive neurons in multiple preparations using the $CCAP^{Gal4AD}$ line with the greatest fidelity to create a "consensus expression pattern" as shown in Figure 3D. Comparison of this pattern with the corresponding consensus expression pattern for the CCAP-Gal4 driver line (Figure 3B) reveals only slight deviations, with the Split Gal4 cross failing to label two CCAP-expressing neurons in the final abdominal segment.

Gal4 transcriptional activity is regulated in yeast by the Gal80 repressor, which binds to a motif included within the Gal4AD (Ma and Ptashne, 1987a). As shown in Figure S2, Gal80 also efficiently suppresses reporter transgene expression in $elav^{Gal4DBD} \cap CCAP^{Gal4AD}$ crosses when coexpressed under control of the CCAP promoter. The Gal4AD-based implementation of the

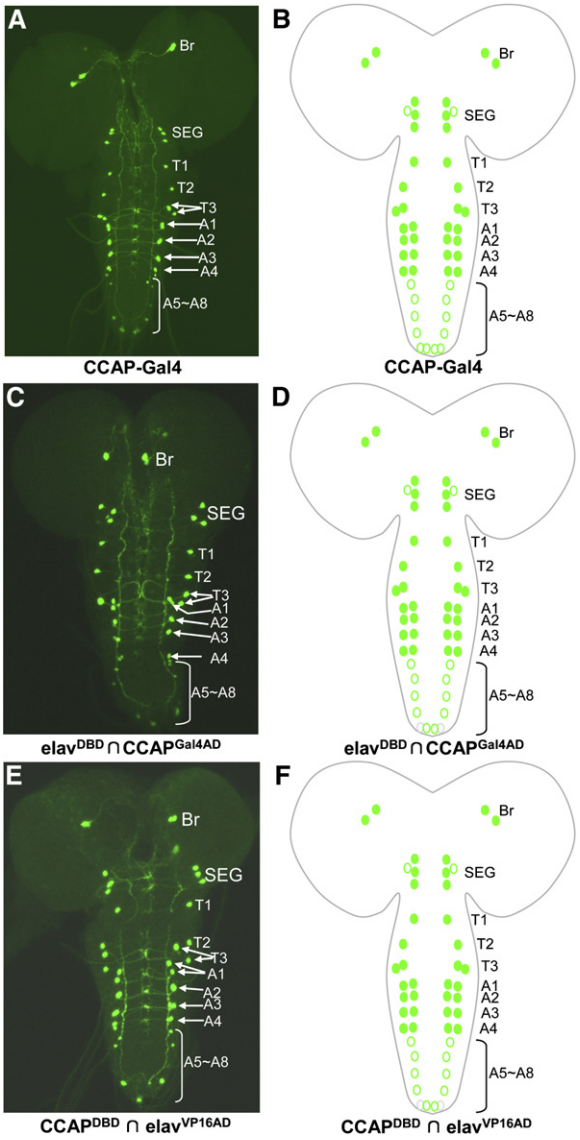

Figure 3. The Split Gal4 System Restricts UAS-Transgene Expression to the Intersection of the Expression Patterns of Two Promoters

Comparison of UAS-EGFP expression in the CNS of third-instar larvae driven by (A and B) CCAP-Gal4 or (C–F) combined Split Gal4 hemidrivers made with the panneuronal elav promoter and the promoter for the CCAP gene. (A) UAS-EGFP expression pattern of CCAP-Gal4 driver. This pattern consists of 48 neurons that express the neuropeptide CCAP. (B) Consensus expression pattern derived from analysis of six preparations like the one shown in (A), as described in Experimental Procedures. (C and D) UAS-EGFP expression pattern driven by $elav^{Gal4DBD} \cap CCAP^{Gal4AD}$ and the corresponding consensus pattern (n = 6). (E and F) UAS-EGFP expression pattern driven by $CCAP^{Gal4DBD} \cap elav^{VP16AD}$ and the corresponding consensus pattern (n = 5). Consensus pattern symbols: circles, the canonical CCAP-expressing neurons, showing their anatomical positions in the CNS (Br, brain; SEG, subesophageal ganglion; T1–3, the three thoracic ganglia; A1–A8, the eight abdominal ganglia); green circles, neurons that expressed EGFP in greater than two-thirds of the preparations; gray circles (see A8 in [D] and [F]), neurons that expressed EGFP in less than two-thirds of preparations. Solid green circles, high EGFP expression; open green circles, low EGFP expression. A few "ectopically" labeled CCAP-immunonegative cells were observed for each driver or hemidriver combination. Their average number per preparation (±SD) was 3 ± 2 (B), 4 ± 2 (D), and 2 ± 2 (F).

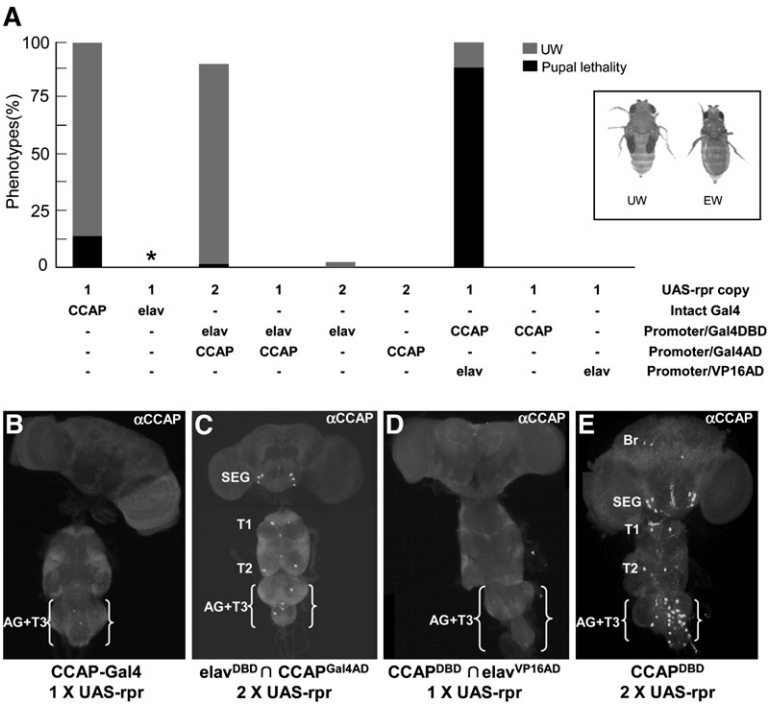

Figure 4. Genetic Ablation of N_{CCAP} Neurons Using the Split Gal4 System Causes Pupal Lethality and Wing-Expansion Deficits that Correlate with Expression Strength

(A) Cumulative percentage of progeny displaying the pupal lethal (black bars) and unexpanded wing (gray bars) phenotypes, following ablation of neurons within the CCAP expression pattern by targeted expression of one or two copies of the cell death gene *reaper* using the indicated driver or combination of hemidrivers. If these phenotypes were not present, no bar is shown. *, embryonic or early larval lethality. (Inset) Adult wing phenotypes. (Left) Unexpanded wings of a newly emerged adult fly. (Right) Same fly after expanding its wings. Adult flies lacking the CCAP-expressing neurons permanently retain the unexpanded wing phenotype.

(B–E) Confocal micrographs of CCAP-immunoreactive neurons in the nervous systems of pharate adult flies expressing UAS-*reaper* driven by the indicated drivers or hemidriver combinations. (B) CCAP-Gal4, (C) $elav^{Gal4DBD}$ and $CCAP^{Gal4AD}$, (D) $CCAP^{Gal4DBD}$ and $elav^{VP16AD}$, and (E) $CCAP^{Gal4DBD}$ alone. The CCAP-immunopositive neurons shown survived the developmental expression of *reaper*. The average number of surviving N_{CCAP} neurons (±SD) in preparations like those shown in panels (B)–(E) were 6.6 ± 0.9 (n = 5), 15.3 ± 1.5 (n = 9), 0 ± 0 (n = 4), and 47.6 ± 0.5 (n = 5), respectively. Abbreviations as in Figure 3, except AG, fused abdominal ganglion of the pharate adult CNS. On average, the pharate adult AG has two fewer N_{CCAP} neurons than are found in the larval abdominal ganglia. Also, the identity of N_{CCAP} neurons in the pharate adult brain is unlikely to correspond to those found in the larval brain.

Split Gal4 system can thus be used in conjunction with the increasing number of transgenic Gal80-expressing fly lines, further extending the range of application of the technique. In particular, coupling the Split Gal4 technique to the TARGET system (McGuire et al., 2003), which exploits a temperature-sensitive Gal80 mutant to temporally regulate Gal4 activity, should permit conditional, as well as spatially restricted, expression of genes of interest.

Restricted expression of the UAS-EGFP reporter within N_{CCAP} was also achieved with the VP16AD construct. The most faithful expression pattern was observed in $CCAP^{Gal4DBD} \cap elav^{VP16AD}$ crosses, when expression of the Gal4DBD domain was anchored to N_{CCAP} (Figure 3E and Figures S1D–S1F). Interestingly, the reciprocal crosses ($elav^{Gal4DBD} \cap CCAP^{VP16AD}$) resulted in expansion of the expression pattern to include numerous neurons outside of N_{CCAP} with all $CCAP^{VP16AD}$ lines tested (Figures S1G–S1I). This infidelity of expression presumably derives from ectopic VP16AD expression and may be the result of a cryptic enhancer in the $CCAP^{VP16AD}$ construct. In any case, it does not affect applications in which precise targeting of the VP16AD hemidriver is unnecessary, such as those using enhancer-trap lines discussed in step 3. However, the possibility of imprecise targeting of this hemidriver must be considered if defined expression of VP16AD is desired.

To further investigate the selectivity of transgene expression driven by Split Gal4 hemidrivers and to confirm the utility of the Split Gal4 system in manipulations of neuronal function, we targeted expression of the cell death gene *reaper* to N_{CCAP} in $elav^{Gal4DBD} \cap CCAP^{Gal4AD}$ and $CCAP^{Gal4DBD} \cap elav^{VP16AD}$ crosses. As shown in Figure 4A, expression of UAS-*reaper* under the control of the elav-Gal4 driver results in early developmental lethality with almost all animals dying at the embryonic or early larval stages. In contrast, *reaper* expression under control of the CCAP-Gal4 driver results in the two developmental phenotypes first described by Park et al. (2003): animals either die as pupae with morphological defects characteristic of head eversion failure, or survive to adulthood without expanding their wings (UW; Figure 4A). Immunohistochemical examination of animals from such crosses shows that *reaper* expression by CCAP-Gal4 typically kills most, but not all, of the CCAP-expressing neurons during development (Figure 4B), whereas control crosses show no neuronal mortality (Figure 4E).

As expected, expression of UAS-*reaper* using the Split Gal4 system led to pupal lethality and wing expansion deficits at levels that correlated with the extent of N_{CCAP} ablation. In addition, the results better define the different efficacies of the two implementations of the Split Gal4 system. Expression of a single copy of the *reaper* transgene in N_{CCAP} using the Split Gal4 system with Gal4AD ($elav^{Gal4DBD} \cap CCAP^{Gal4AD}$) was without effect, but expression of two copies caused wing expansion deficits in 90% of progeny, with little concomitant pupal lethality (Figure 4A). On average, expression of two copies of UAS-*reaper* resulted in the death of approximately two-thirds of the N_{CCAP} neurons (Figure 4C). The Split Gal4 system, implemented with Gal4AD, thus clearly drives reaper expression less potently than intact Gal4, and the absence of the pupal lethal phenotype indicates that the neurons responsible for it were not killed or were killed in insufficient numbers

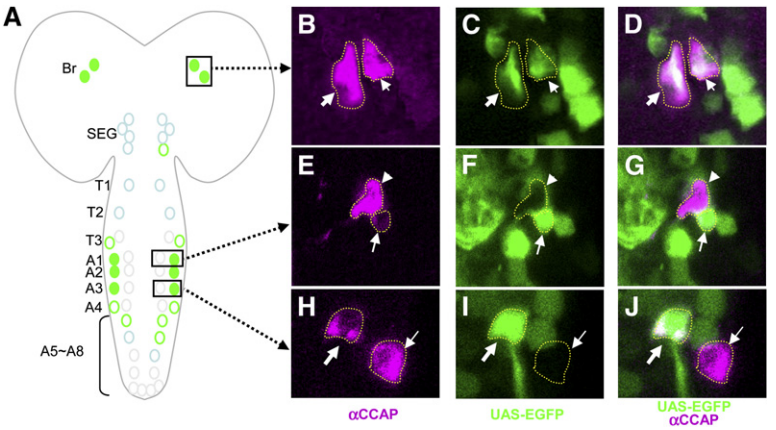

Figure 5. A Subset of N_{CCAP} Neurons Is Cholinergic and Lies within the Expression Pattern of the Choline Acetyltransferase Promoter

(A) Consensus labeling pattern showing the overlap of Cha-Gal4 expression (detected with UAS-EGFP) with N_{CCAP} (detected by anti-CCAP immunolabeling; n = 9). Circles, CCAP-immunopositive neurons. Green circles, EGFP labeled in greater than one-third of the preparations. Light-blue circles, EGFP labeled in one-third or less of the preparations. Gray circles, neurons that were never EGFP labeled. Filled circles, consistently high EGFP expression (see Experimental Procedures). Open circles, low EGFP expression. In paired N_{CCAP} neurons in hemisegments T3–A4, one was typically strongly CCAP immunopositive and the other was more weakly labeled. For convenience, we have shown the strongly expressing neuron as medial to the weakly expressing one. This does not necessarily represent their anatomical positions. (B–J) High-resolution confocal micrographs showing anti-CCAP immunoreactivity (B, E, and H), EGFP expression (C, F, and I), and their overlap (D, G, and J). For each set of images, individual neurons are indicated by arrows and dotted outlines. Boxes in (A) show the anatomical location of the corresponding images. In hemisegments T3 and A1–A4, only the more weakly CCAP-immunoreactive neuron of the pair expresses EGFP.

even by two copies of the UAS-*reaper* transgene. In contrast, expression of a single copy of the reaper transgene in $CCAP^{Gal4DBD} \cap elav^{VP16AD}$ crosses resulted in nearly complete pupal lethality (Figure 4A) and the death of almost all N_{CCAP} neurons (Figure 4D), indicating that this implementation of the Split Gal4 system drives *reaper* expression more potently than intact Gal4. These results are consistent with the levels of EGFP reporter gene expression seen using the two implementations of the system (see Figures 2F–2H). Control crosses expressing single hemidrivers and one or two copies of the *reaper* transgene produced progeny without pupal mortality or significant wing expansion deficits (Figure 4A). Overall, our results indicate that the Split Gal4 system drives *reaper* expression in N_{CCAP} at levels sufficient to ablate some or all of these neurons, with VP16AD providing considerably more potent transgene expression than Gal4AD.

Step 3: The Split Gal4 System Can Target Gene Expression to the Intersection of Two Overlapping Expression Patterns (P_1 Overlaps P_2)

The greatest utility of the Split Gal4 system lies in its potential to limit transgene expression to the intersection of two distinct but overlapping expression patterns. We describe here an example of this application using two defined promoters. The next section describes a second example using hemidrivers made with undefined promoters (i.e., enhancer-trap lines) to drive gene expression at the intersection of two patterns.

The Gal4AD, with its high degree of fidelity when expressed under a specific promoter, is particularly useful when both the AD and Gal4DBD hemidrivers must be faithfully targeted. We used the $CCAP^{Gal4AD}$ in conjunction with a Gal4DBD hemidriver made with the choline acetyltransferase (Cha) promoter (Salvaterra and Kitamoto, 2001) to selectively drive transgene expression in cholinergic N_{CCAP} neurons. Preliminary immunohistochemical studies indicated that at least some N_{CCAP} neurons were cholinergic, and to provide a baseline for assessing the fidelity of $Cha^{Gal4DBD} \cap CCAP^{Gal4AD}$-driven expression, we determined the consensus pattern of Cha promoter activity within N_{CCAP} immunohistochemically (Figure 5A). As indicated in Figure 5, certain CCAP-immunopositive neurons, such as the bilaterally represented pairs in the brain (Figures 5A and 5B–5D), are consistently double labeled in Cha-Gal4 > UAS-EGFP preparations. In the ventral nerve cord, the more-weakly immunopositive member of the pair of CCAP-expressing neurons in hemisegments A1–A4 is also often EGFP labeled, as shown in the examples of Figures 5E–5J, while the strongly immunopositive member of this pair is never EGFP labeled. In general, we observed considerable variability in the pattern of overlap, suggesting extensive variability of the Cha-Gal4 expression within N_{CCAP}, but the consensus labeling pattern (Figure 5A), derived from nine double-labeled preparations, shows that 18 of the 48 N_{CCAP} neurons are found within the Cha-Gal4 pattern in greater than a third of the preparations, while 13 other neurons are found double labeled at lower frequency.

Figure 6 shows the corresponding results obtained with the Split Gal4 system, in which UAS-EGFP expression was driven by $Cha^{Gal4DBD} \cap CCAP^{Gal4AD}$ (Figures 6A–6C). Whole mounts of the CNS from these animals were stained with anti-CCAP antibody (Figure 6D) to positively identify each EGFP-labeled neuron, and a consensus expression pattern was determined from the examination of multiple animals (Figure 6I). As with the Cha-Gal4 driver, and therefore unsurprisingly, there was considerable variability in the expression pattern, but in all preparations almost all EGFP-expressing neurons were also CCAP immunopositive (Figure 6D), and there was good correspondence in the two consensus expression patterns (compare Figure 6I with Figure 5A). In particular, the neurons most frequently observed in the Split Gal4 pattern were the CCAP-immunopositive neurons of the brain (Figure 6D, arrowheads) and specific hemisegmentally represented neurons in the ventral nerve cord (Figure 6D, box). Just as observed with the Cha-Gal4 driver, the latter neurons in hemisegments A1–A4 corresponded to the weakly

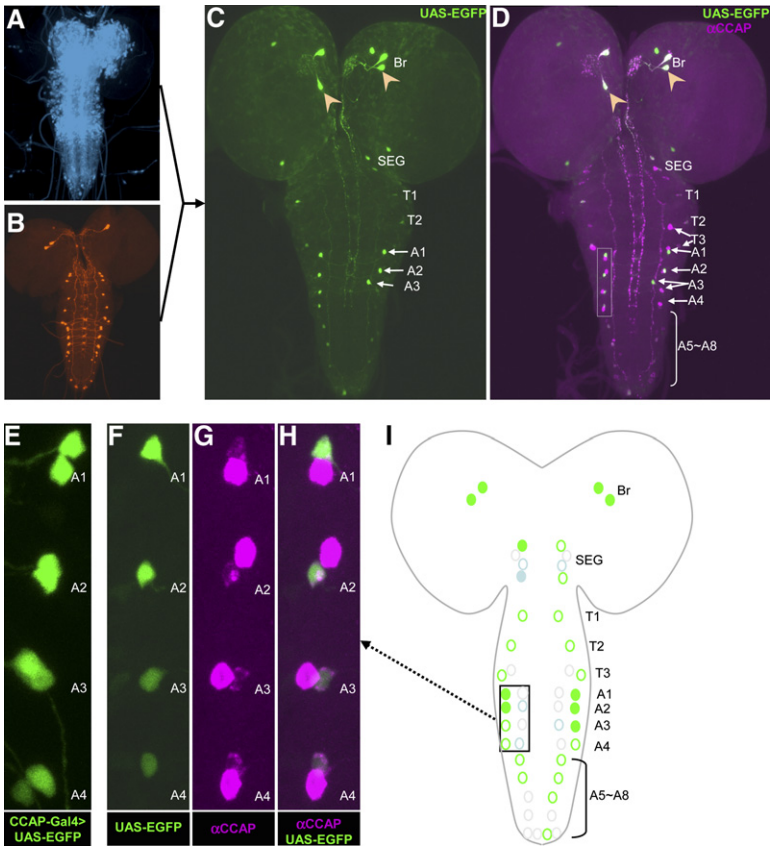

Figure 6. Targeting the Cholinergic Subset of N_{CCAP}, Using Complementary Hemidrivers Made with the Cha and CCAP Promoters

The pattern of UAS-EGFP expression in the CNS of *Drosophila* third-instar larvae driven by the Split Gal4 hemidrivers $Cha^{Gal4DBD}$ and $CCAP^{Gal4AD}$. (A and B) Expression patterns of the promoters used to make the $Cha^{Gal4DBD}$ and $CCAP^{Gal4AD}$ hemidriver lines. (A) Cha-Gal4 > UAS-EGFP (blue pseudocolor). (B) CCAP-Gal4 > UAS-EGFP (red pseudocolor). (C and D) Restricted pattern of UAS-EGFP expression within N_{CCAP} in $Cha^{Gal4DBD} \cap CCAP^{Gal4AD}$ crosses. (C) A representative example of EGFP expression. (D) Both EGFP expression (green) and CCAP immunostaining (magenta) in sample from (C). Anatomical abbreviations are as in Figure 3. Consistently double-labeled neurons in the brain (arrowheads) and in hemisegments A1–A4 (box in [D]) are indicated. (E) UAS-EGFP driven by CCAP-Gal4 expresses in both strong and weak CCAP-immunoreactive cells of hemisegments A1–A4. (F–H) Higher-magnification images of the boxed region in (D) showing restriction of EGFP expression to only the more weakly immunoreactive N_{CCAP} neuron of the pair in hemisegments A1–A4. (F) UAS-EGFP expression. (G) CCAP immunolabeling. (H) Merged image of (F) and (G). (I) Consensus pattern of UAS-EGFP expression driven by $Cha^{Gal4DBD} \cap CCAP^{Gal4AD}$, derived from seven preparations. The average frequency and intensity of labeling for each identified neuron are designated as in Figure 5. Boxed region, hemisegments A1–A4 shown in (F)–(H). Ectopically labeled neurons are not represented in the consensus pattern. On average, 7 ± 2 (n = 7) non-CCAP-immunoreactive cells were observed per preparation. Some of these, such as the two in the brain, appear to correspond to cells also sometimes seen in CCAP-Gal4 labeling patterns.

CCAP-immunopositive neuron of a pair (Figures 6F–6I, box), both of which are equally well labeled by CCAP-Gal4 (Figure 6E).

Restriction of Gene Expression to Arbitrary Subsets of Cells within a Group of Interest Using VP16AD Enhancer-Trap Hemidrivers

Another strategy for restricting expression within a pattern of interest, particularly useful when there are no known promoters with overlapping expression patterns, uses enhancer-trap lines (Bellen et al., 1989) to express the complementary hemidriver. Enhancer-trap constructs are made with a minimal promoter and express in "arbitrary" patterns dictated by local enhancer elements near the site of transgene integration into the genome. Because the fidelity of expression of the enhancer-trap construct is immaterial, the VP16AD, with its potential for driving transgene expression at high levels, is useful for this application. We therefore made enhancer-trap lines with the VP16AD construct (ET^{VP16AD}) and selected those with expression patterns that overlapped with N_{CCAP}. The broad expression patterns of two such lines (ET^{VP16AD}-N4 and ET^{VP16AD}-N6), revealed by crosses to $elav^{Gal4DBD}$, are shown in Figures 7A and 7C, respectively. The restricted patterns of expression within N_{CCAP} (Figure 7B), generated by crosses of these lines to $CCAP^{Gal4DBD}$, are shown in Figures 7D and 7F, respectively. As is evident from their consensus expression patterns (Figures 7E and 7G), the two enhancer-trap hemidrivers limit expression to two nearly mutually exclusive subsets of N_{CCAP}. ET^{VP16AD}-N4 crosses to $CCAP^{Gal4DBD}$ drive expression almost exclusively in neurons of the subesophageal and thoracic ganglia, while those of ET^{VP16AD}-N6 drive expression primarily in the brain and abdominal ganglia.

Dissection of Neural Network Function Using the Split Gal4 System

Having identified enhancer-trap lines capable of selectively expressing transgenes in discrete subsets of N_{CCAP}, we next used them to probe the functional identities of the neurons within this group. As indicated above, N_{CCAP} plays a critical role in wing expansion in the early adult, and we wished to determine which neurons within this group might be necessary and/or sufficient for this process. We therefore ablated the subsets of N_{CCAP} neurons included in the ET^{VP16AD}-N4 and ET^{VP16AD}-N6 expression patterns using UAS-*reaper* and correlated the patterns of the surviving N_{CCAP} neurons with the wing-expansion phenotype.

We used anti-CCAP immunostaining of the nervous system to assess the patterns of surviving N_{CCAP} neurons (Figures 8A and 8E). Because the CCAP-expressing neurons apoptose shortly after eclosion (Draizen et al., 1999), it was necessary to evaluate the patterns of the surviving N_{CCAP} neurons in pharate adults, that is, at

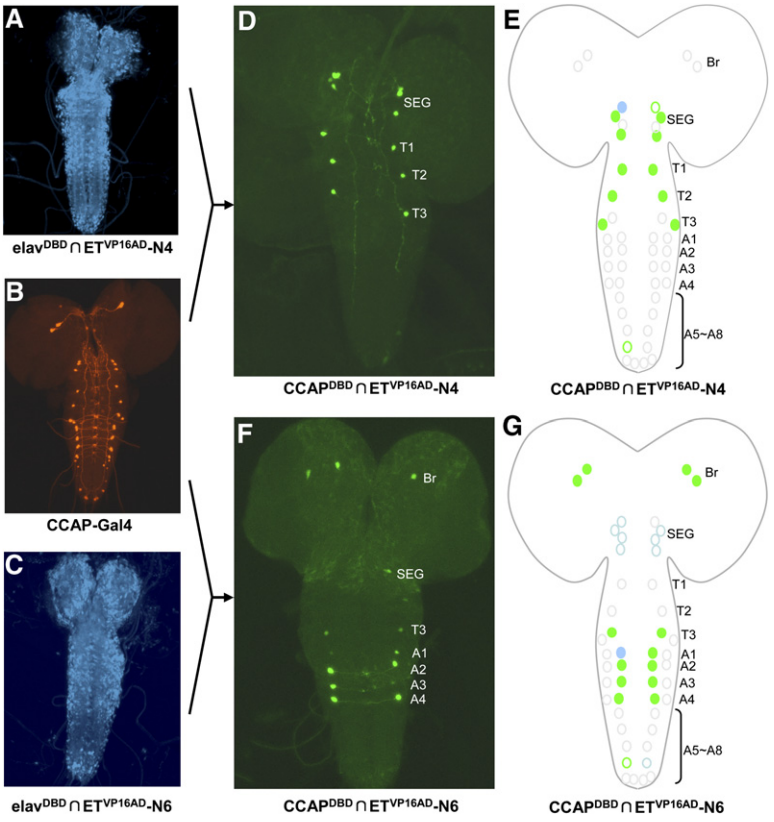

Figure 7. Split Gal4 Enhancer-Trap Lines Can Be Used to Target Distinct Subsets of Neurons within N_{CCAP}

Patterns of EGFP expression in the CNS of *Drosophila* third-instar larvae driven by the $CCAP^{Gal4DBD}$ hemidriver combined with two different VP16AD enhancer trap lines. (A–C) Expression patterns of two VP16AD enhancer-trap hemidrivers and CCAP-Gal4. Nervous system expression (blue pseudocolor) of (A) the ET^{VP16AD}-N4 and (C) ET^{VP16AD}-N6 enhancer-trap lines revealed by combining them with the $elav^{Gal4DBD}$ hemidriver in the presence of a UAS-EGFP reporter. (B) CCAP-Gal4 > UAS-EGFP. (D–G) Restricted patterns of UAS-EGFP expression generated by (D) $CCAP^{Gal4DBD} \cap ET^{VP16AD}$-N4, and (F) $CCAP^{Gal4DBD} \cap ET^{VP16AD}$-N6, and (E and G) their corresponding consensus patterns. Consensus patterns were derived from four ET^{VP16AD}-N4 and six ET^{VP16AD}-N6 double-labeled preparations, respectively, with neurons represented as in Figure 5.

a stage just before eclosion and wing expansion. Therefore, we could not compare wing expansion with the surviving N_{CCAP} neurons in individual animals. To help identify these neurons, which differ somewhat in number and position from those of the larval stage, we double labeled the preparations with an antibody to the hormone bursicon (Figures 8B–8C, 8F, and 8G), which is expressed in a subset of N_{CCAP}, including 14 neurons in the abdominal ganglion (Figure 8I). Ablations performed using the ET^{VP16AD}-N4 hemidriver primarily affected neurons of the subesophageal and thoracic ganglia (Figure 8D, black circles), as expected from the expression pattern in third-instar larvae (Figure 7E). Six abdominal ganglion neurons that appear in the expression pattern only during pupal development (data not shown), and which do not express bursicon, were also ablated. In contrast, ablations performed using the ET^{VP16AD}-N6 hemidriver mostly spared the neurons of the thoracic and subesophageal ganglia, but eliminated, on average, 12 of the 30 abdominal ganglion neurons, including nine that express bursicon (Figure 8H). Interestingly, only ablations performed with the ET^{VP16AD}-N4 hemidriver yielded animals that failed to expand their wings (Figure 8J). This effect was not fully penetrant, but because there were slight variations in the patterns of cell death from animal to animal (see Figure 8C, legend), it is likely that the 15% of animals that expanded their wings normally corresponded to those in which some small number of critical neurons were not killed.

The two lines therefore identify functionally, as well as anatomically, distinct subsets of N_{CCAP}. The set of neurons surviving the ablation with ET^{VP16AD}-N6 (Figure 8H, red) is clearly sufficient to support wing expansion, and the set surviving ablation with ET^{VP16AD}-N4 (Figure 8D, red) is insufficient for wing expansion. Conversely, some or all of the neurons ablated in crosses using ET^{VP16AD}-N4 (Figure 8D, black circles) must be necessary for wing expansion. If we remove from this latter group the small number of neurons that are clearly unnecessary, because they are ablated without effect in ET^{VP16AD}-N6 crosses (e.g., the middle pair of subesophageal neurons), we are left with a minimal subset of neurons, some or all of which must be necessary for wing expansion (Figure 8K, red).

This "critical subset" represents part of a larger group of previously identified neurons, and our results with the Split Gal4 system confirm and extend an earlier model of N_{CCAP} function. Previously, we showed that neurons within N_{CCAP} act as a small network with output and regulatory functions, both of which are necessary for wing expansion (Luan et al., 2006). The critical subset identified here (Figures 8K–8L, red filled) definitively implicates several neurons within the broad group previously identified as candidate regulatory neurons as required for wing expansion (Figure 8L, blue circles). However, as can be seen in Figure 8L, the critical subset cannot be sufficient for wing expansion, since it does not include any of the 14 bursicon-expressing neurons that comprise the output group (green circles). As shown in Figure 8H, ablation of up to nine of the bursicon-expressing neurons with ET^{VP16AD}-N6 does not compromise wing expansion, suggesting that some or all of the remaining five bursicon-expressing neurons are necessary. Alternatively, it is possible that the output

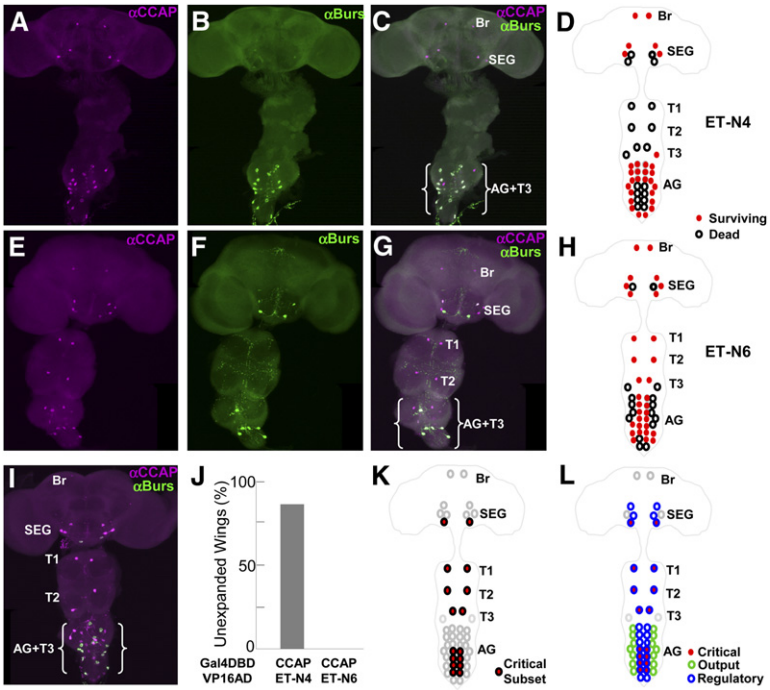

Figure 8. Genetic Ablation of Neurons within N_{CCAP} Using the Split Gal4 System Identifies Anatomically and Functionally Distinct Subsets of This Network

(A–D) Pattern of N_{CCAP} neuronal survival after ablation by UAS-*reaper*, driven by $CCAP^{Gal4DBD} \cap ET^{VP16AD}$-N4. (A) Confocal image showing surviving CCAP-immunopositive cells in the CNS of a pharate adult. (B) Pattern of bursicon immunoreactivity in the same double-labeled preparation. (C) Merged image of (A) and (B). The average number of surviving N_{CCAP} neurons (±SD) from seven preparations was 30.3 ± 2.1. (D) Consensus pattern of surviving (red filled circles) and ablated (black open circles) N_{CCAP} neurons. Note that ET^{VP16AD}-N4 expression within N_{CCAP} changes developmentally so that more neurons are killed than are seen in the larval CNS expression pattern (Figure 7E). ET-N4, enhancer-trap line ET^{VP16AD}-N4.

(E–H) N_{CCAP} neuronal survival after ablation by UAS-*reaper*, driven by $CCAP^{Gal4DBD} \cap ET^{VP16AD}$-N6, similar to (A)–(D). The average number of surviving N_{CCAP} neurons (±SD) from eight preparations was 32.9 ± 5.6. ET-N6, enhancer-trap line ET^{VP16AD}-N6.

(I) The patterns of anti-CCAP (magenta) and anti-bursicon (green) labeling in the CNS of a control animal are shown for comparison. The pharate adult CNS typically has 48 N_{CCAP} neurons, including 14 bursicon-immunopositive neurons in the AG and one or two pairs in the SEG.

(J) Percentage of progeny with unexpanded wings in crosses with UAS-*reaper* driven by $CCAP^{Gal4DBD} \cap ET^{VP16AD}$-N4 and $CCAP^{Gal4DBD} \cap ET^{VP16AD}$-N6. Gray bar shows the frequency of the unexpanded wing phenotype. No bar denotes normally expanded wings.

(K) A critical subset (red filled black circles) of neurons within N_{CCAP}, some or all of which must be necessary for wing expansion. This subset includes all neurons ablated in crosses with ET^{VP16AD}-N4 that were not also ablated in crosses with ET^{VP16AD}-N6. Neurons ablated with ET^{VP16AD}-N6 are clearly not necessary for wing expansion since flies from crosses with this hemidriver showed normal wing expansion. The critical set does not contain any of the bursicon-expressing neurons in the AG. Because the identities of the non-bursicon-expressing neurons in the abdominal ganglion are difficult to determine, it is unclear whether the subset of AG neurons ablated using ET^{VP16AD}-N4 overlaps with the subset ablated using ET^{VP16AD}-N6. We have therefore included all ablated abdominal ganglion neurons from (D) in the critical set.

(L) Schematic of N_{CCAP} comparing the critical set of N_{CCAP} neurons (red fill) defined in (K), with previously identified candidate output (green open circles) and regulatory (blue open circles) neurons within the N_{CCAP} network (Luan et al., 2006). The critical set identifies a subset of the previous, broadly defined regulatory group as important for wing expansion.

function is distributed and that various subsets of the output group are sufficient to promote wing expansion. Although further work with other enhancer-trap lines and other effectors will be required to elucidate the individual functional identities of neurons within N_{CCAP}, this example illustrates how the Split Gal4 system can be used to systematically subdivide and define the functional elements of a neuronal circuit.

Conclusions

The Split Gal4 technique introduced here is a general and versatile method for targeting transgene expression to subsets of neurons within a pattern of interest. Because it uses the Gal4DBD, it is compatible with the hundreds of UAS-effector lines already available in *Drosophila*. Its implementation using the Gal4AD also makes it compatible with the growing number of Gal80 lines and permits an additional level of spatial or temporal control. The two implementations of the technique presented have complementary strengths. The Gal4AD, although weaker than the VP16AD, can drive effector transgene expression at levels sufficient to manipulate neuronal viability and function and can be targeted with high fidelity when used with specific promoters. The VP16AD, as we have shown, is better suited for use in enhancer-trap constructs where its lower promoter fidelity is unproblematic and its higher transcriptional activity permits even weak effector transgenes to be used at single-copy dosages. Although expression of the VP16AD together with the GalDBD may be toxic in a small population of neurons, as evidenced by the general lethality of panneuronal expression, such toxicity is clearly not the rule, as we have not observed it in any other application, including applications using VP16AD enhancer trap lines with broad expression in the nervous system (Figures 7A and 7C).

We have demonstrated the utility of the Split Gal4 technique in the field of neuronal circuit analysis, where we expect it will find fertile application. It should be possible to use the technique not only to subdivide known neuronal groups but also to perform screens analogous to current Gal4 enhancer-trap screens to identify as yet unknown neuronal substrates of physiological processes or behaviors. Unlike current screens, however, it should be possible to use the Split Gal4 technique iteratively, to successively refine the identification of neuronal substrates within a group of interest once it is identified, as outlined in Figure S3. The level of resolution attainable with the Split Gal4 system may vary depending on the homogeneity of gene expression in the cell group of interest, but given the high degree of neuronal specialization normally observed, this is unlikely to be a major limitation. We also anticipate that the usefulness of the Split Gal4 system introduced

here will extend beyond the nervous system to other tissues and other fields of research. Finally, while we have implemented the Split Gal4 technique in *Drosophila*, there is no reason it cannot be implemented in other genetic model organisms, such as zebrafish or mice, where similar transcriptional systems for the expression of foreign genes exist.

Experimental Procedures

Generation of Optimized Hemidriver Constructs

The optimized Gal4DBD, Gal4AD, and VP16AD constructs used for in vitro testing were assembled between the EcoRV and HpaI restriction sites (Figure S4A) in the pActPL vector (Wei et al., 2000) using PCR fragments corresponding to the transcription factor, polyglycine linker, and the heterodimerizing leucine zipper domains. Transcription factor PCR templates were made to pGBKT7 (Clontech), pGADT7 (Clontech), and pUHD15-1 (Resnitzky et al., 1994) and were designed to amplify sequences encoding amino acids 1–147 (Gal4DBD) and 768–881 (Gal4AD) of Gal4, and 413–490 (VP16AD) of VP16, respectively. The heterodimerizing leucine zipper domains corresponded to the $RR_{12}EE_{345}L$ (Zip^{-}) and $EE_{12}RR_{345}L$ (Zip^{+}) sequences described by Moll et al. (2001) and were generated from synthetic oligonucleotides with codon usage optimized for *Drosophila* expression. A point mutation inadvertently introduced by PCR resulted in a Y → N mutation at amino acid 36 in the $EE_{12}RR_{345}L$ domain used in the Gal4AD and VP16AD constructs. The transcription factor sequences of all pActPL constructs are flanked by unique restriction sites at the 5′ (NotI) and 3′ (AscI) ends.

Generation of Transformation Vectors and Transgenic Fly Lines

The $elav^{Gal4DBD}$, $elav^{Gal4AD}$, and $elav^{VP16AD}$ transformation constructs used to make transgenic flies were made from the pCaST vector as described in Figure S4B. This vector was derived from pP{elav-GeneSwitch} (Osterwalder et al., 2001) by replacing an EcoRI-XbaI fragment containing the elav-promoter and GeneSwitch sequences with a polylinker containing EcoRI-BglII-NotI-AscI-XbaI restriction sites to make pCaST. The $Cha^{Gal4DBD}$, $CCAP^{Gal4DBD}$, $CCAP^{Gal4AD}$, and $CCAP^{VP16AD}$ transformation constructs were generated from a derivative of pCaST, called X11 (Figure S4C), which was made by replacing the EcoRI-elav-NotI fragment of pCaST-$elav^{Gal4DBD}$ with a polylinker containing EcoRI-AvrII-BglII-PmeI-NotI sites. The enhancer trap constructs ET^{Gal4AD} and ET^{VP16AD} were made by inserting NotI-Gal4AD-AscI and NotI-VP16AD-AscI fragments into pEG117 (Giniger et al., 1993), after replacing the KpnI site in the polylinker of this vector by AscI (Figure S4D).

Generation and Characterization of Transgenic Fly Lines

P element injections and isolation of transformants were performed for all plasmids by Genetic Services, Inc. Six to fourteen independent lines were made for each construct, and the chromosomal locations of the transgenes were determined by segregation analysis. In step 1, a UAS-EYFP or UAS-EGFP transgene was introduced into the $elav^{Gal4DBD}$ lines, and these lines were crossed pairwise with $elav^{Gal4AD}$ and $elav^{VP16AD}$ lines to determine viability and fluorescence expression levels of the progeny. Of the ten $elav^{Gal4DBD}$ lines we made, only one ($elav^{Gal4DBD}$-H9) yielded viable adult progeny in pairwise crosses to $elav^{VP16AD}$ hemidrivers. Crosses made with the other nine lines died as embryos or early larvae. Neither the pattern nor levels of fluorescence in these embryos differed overtly from those observed in embryos from viable crosses, and in all cases the fluorescence intensity was very high. The mortality is unlikely to be due either to toxicity of the highly expressed reporter, since identical crosses lacking a UAS-transgene also failed to yield viable progeny, or to transcriptional squelching (Cahill et al., 1994), since animals expressing only the $elav^{VP16AD}$ construct are viable and healthy.

Transgenic lines generated in steps 2 and 3 were characterized similarly to those generated in step 1. Consensus expression patterns were derived for at least two independent $CCAP^{Gal4DBD}$, $CCAP^{Gal4AD}$, and $CCAP^{VP16AD}$ lines by multiple pairwise crosses to complementary panneuronal hemidrivers. Independent lines expressing the same construct had similar consensus patterns in all cases. In step 3, consensus patterns were determined for three independent $Cha^{Gal4DBD}$ lines in pairwise crosses to two independent $CCAP^{Gal4AD}$ lines.

Other Fly Stocks

The Gal4 driver and UAS-reporter/effector lines used in this study: *yw; +*; *CCAP-Gal4* (Park et al., 2003); *yw; UAS-2XEGFP; UAS-2XEGFP* (Halfon et al., 2002), and *yw; +; elav-Gal4* (Luo et al., 1994); *w; Cha-Gal4-19B; +* (Salvaterra and Kitamoto, 2001). The *w; rpr; +* and Canton-S lines were from the Bloomington Stock Center. *yw; CCAP-Gal80; Dr/TM3,Sb* (ET1-B1A) is a second chromosome insert of the construct described in Luan et al. (2006). All flies were raised on standard corn meal-molasses medium and maintained at 25°C/65% relative humidity on a constant 12 hr light/dark cycle.

Cell Culture, Transfection, and β-Galactosidase Activity Measurement

Drosophila SL2 cells were cultured and transfected according to previously described methods (Wei et al., 2000). For each measurement, 2×10^6 cells were transfected 24 hr after plating using Fugene 6 (Roche Diagnostics) and 2 μg of plasmid(s). Plasmids included pActPL vectors containing the intact Gal4, Gal4DBD, Gal4AD, and/or VP16AD transcription factor constructs, together with a UAS-nucLacZ reporter plasmid. The pRmHa3′ vector was used as a carrier when necessary to insure addition of the same amount of DNA in all transfections. Seventy-two hours after transfection, cells were lysed and β-galactosidase activity was quantified using the β-gal Reporter Gene Assay, Chemiluminescent Kit (Roche Diagnostics).

Immunohistochemistry and Microscopy

Wandering third-instar larvae or late-stage, black-winged pharate adults were dissected in PBS, and the excised nervous systems were fixed, permeabilized, and stained as described previously (Luan et al., 2006). Antibody labeling was carried out with rabbit anti-CCAP (Ewer and Truman, 1996) at 1:5000 dilution, and mouse anti-bursicon β-subunit (Luo et al., 2005) at 1:250 dilution. Alexa Fluor 488-coupled goat-anti-rabbit and Alexa Fluor 596-coupled goat-anti-mouse fluorescent secondary antibodies were from Invitrogen. Whole-mount preparations were imaged with a Nikon C-1 confocal microscope. Optical sections were acquired using a 20× objective or 40× objective for all figures except the high-resolution images of anti-CCAP immunostaining shown in Figures 5B–5J and 6E–6H, which were acquired using a 60× oil-immersion objective. All images of the brain and ventral nerve cord are volume-rendered Z stacks.

Analysis of Expression Patterns and Immunoreactivity

UAS-EGFP expression driven by intact Gal4 or by Split Gal4 hemidrivers varied somewhat between individuals. To represent the frequency and intensity of UAS-EGFP expression in individual identified N_{CCAP} neurons, we created consensus expression patterns derived from multiple CNS preparations of each genotype. Each image from the confocal Z stack containing a CCAP-immunopositive neuronal soma was then evaluated for overlapping UAS-EGFP expression. The intensity (I) of labeling of each soma was scored on a scale of 0–3. The consensus intensity value for each identified CCAP-expressing neuron was calculated by averaging all values for this neuron across preparations. In the consensus patterns for third-instar larvae, cells with average values of $I \geq 2$ are represented as filled circles. Open circles have average values of $0 < I < 2$. The frequency with which each neuron expressed EGFP was equal to the number of preparations in which $I \neq 0$ for that neuron divided by the total number of preparations, and is represented as described in the figure legends.

For experiments in which *reaper* was used to ablate CCAP-expressing neurons, the number and identity of the surviving cells were determined by examining anti-CCAP and/or anti-bursicon-labeled preparations imaged by confocal microscopy. Surviving neurons in each preparation were counted and the means and standard deviations calculated for all preparations within an experiment. In the consensus patterns of Figure 8, a cell is represented as "ablated" if it was present in less than one-third of the samples.

Analysis of Lethality and Wing Expansion Phenotypes

The UAS-*reaper* transgene used for genetic ablation in this paper is less potent than the one used previously by Park et al. (2003) and was selected to better distinguish the relative efficacies of the Gal4AD and VP16AD hemidrivers. In ablation experiments, wing phenotypes were scored as described in Luan et al. (2006), at least 24 hr after eclosion to ensure that the final phenotype had been attained. Pupal mortality was assessed 7 days after a cross had been terminated and all live animals had eclosed, by dividing the number of dead pupae by the total number of live progeny plus dead pupae generated by the cross.

Supplemental Data

The Supplemental Data for this article can be found online at http://www.neuron.org/cgi/content/full/52/3/425/DC1/.

Acknowledgments

We would like to acknowledge John Ewer, Cahir O'Kane, Haig Keshishian, Toshihiro Kitamoto, and the Bloomington Stock Center for providing fly stocks, and the National Institute of Neurological Disorders and Stroke sequencing facility for services. We also thank Paul Salvaterra, Jae Park, Ed Giniger, Bruce Patterson, Chi-hon Lee, and Marc Halfon for plasmids, and John Ewer and Aaron Hsueh for antibodies. Bruce Paterson also kindly provided cell lines. We also express our appreciation to Grace Gray, Chi-hon Lee, and Harold Gainer for comments on the manuscript, and to Howard Nash who provided sound advice and enthusiastic encouragement throughout the project. This research was supported by the Intramural Research Programs of the National Institute of Mental Health (B.H.W) and the National Cancer Institute (C.R.V.), NIH.

Received: March 16, 2006
Revised: July 13, 2006
Accepted: August 17, 2006
Published: November 8, 2006

References

Awatramani, R., Soriano, P., Rodriguez, C., Mai, J.J., and Dymecki, S.M. (2003). Cryptic boundaries in roof plate and choroid plexus identified by intersectional gene activation. Nat. Genet. *35*, 70–75.

Bellen, H.J., O'Kane, C.J., Wilson, C., Grossniklaus, U., Pearson, R.K., and Gehring, W.J. (1989). P-element-mediated enhancer detection: a versatile method to study development in Drosophila. Genes Dev. *3*, 1288–1300.

Brand, A.H., and Perrimon, N. (1993). Targeted gene-expression as a means of altering cell fates and generating dominant phenotypes. Development *118*, 401–415.

Brent, R., and Ptashne, M. (1985). A eukaryotic transcriptional activator bearing the DNA specificity of a prokaryotic repressor. Cell *43*, 729–736.

Cahill, M.A., Ernst, W.H., Janknecht, R., and Nordheim, A. (1994). Regulatory Squelching. FEBS Lett. *344*, 105–108.

Draizen, T.A., Ewer, J., and Robinow, S. (1999). Genetic and hormonal regulation of the death of peptidergic neurons in the Drosophila central nervous system. J. Neurobiol. *38*, 455–465.

Duffy, J.B. (2002). GAL4 system in Drosophila: a fly geneticist's Swiss army knife. Genesis *34*, 1–15.

Ewer, J., and Truman, J.W. (1996). Increases in cyclic 3′, 5′-guanosine monophosphate (cGMP) occur at ecdysis in an evolutionarily conserved crustacean cardioactive peptide-immunoreactive insect neuronal network. J. Comp. Neurol. *370*, 330–341.

Farago, A.F., Awatramani, R.B., and Dymecki, S.M. (2006). Assembly of the brainstem cochlear nuclear complex is revealed by intersectional and subtractive genetic fate maps. Neuron *50*, 205–218.

Fassler, J., Landsman, D., Acharya, A., Moll, J.R., Bonovich, M., and Vinson, C. (2002). B-ZIP proteins encoded by the Drosophila genome: Evaluation of potential dimerization partners. Genome Res. *12*, 1190–1200.

Fields, S., and Song, O. (1989). A novel genetic system to detect protein-protein interactions. Nature *340*, 245–246.

Giniger, E., Wells, W., Jan, L.Y., and Jan, Y.N. (1993). Tracing neurons with a kinesin-beta-galactosidase fusion protein. Rouxs Arch. Dev. Biol. *202*, 112–122.

Gossen, M., and Bujard, H. (1992). Tight control of gene expression in mammalian cells by tetracycline-responsive promoters. Proc. Natl. Acad. Sci. USA *89*, 5547–5551.

Halfon, M.S., Gisselbrecht, S., Lu, J., Estrada, B., Keshishian, H., and Michelson, A.M. (2002). New fluorescent protein reporters for use with the Drosophila Gal4 expression system and for vital detection of balancer chromosomes. Genesis *34*, 135–138.

Keegan, L., Gill, G., and Ptashne, M. (1986). Separation of DNA binding from the transcription-activating function of a eukaryotic regulatory protein. Science *231*, 699–704.

Lee, T., and Luo, L. (1999). Mosaic analysis with a repressible cell marker for studies of gene function in neuronal morphogenesis. Neuron *22*, 451–461.

Luan, H., Lemon, W.C., Peabody, N.C., Pohl, J.B., Zelensky, P.K., Wang, D., Nitabach, M.N., Holmes, T.C., and White, B.H. (2006). Functional dissection of a neuronal network required for cuticle tanning and wing expansion in Drosophila. J. Neurosci. *26*, 573–584.

Luo, L., Liao, Y.J., Jan, L.Y., and Jan, Y.N. (1994). Distinct morphogenetic functions of similar small GTPases: Drosophila Drac1 is involved in axonal outgrowth and myoblast fusion. Genes Dev. *8*, 1787–1802.

Luo, C.W., Dewey, E.M., Sudo, S., Ewer, J., Hsu, S.Y., Honegger, H.W., and Hsueh, A.J. (2005). Bursicon, the insect cuticle-hardening hormone, is a heterodimeric cystine knot protein that activates G protein-coupled receptor LGR2. Proc. Natl. Acad. Sci. USA *102*, 2820–2825.

Ma, J., and Ptashne, M. (1987a). The carboxy-terminal 30 amino-acids Of Gal4 are recognized by Gal80. Cell *50*, 137–142.

Ma, J., and Ptashne, M. (1987b). Deletion analysis of Gal4 defines two transcriptional activating segments. Cell *48*, 847–853.

Mallo, M. (2006). Controlled gene activation and inactivation in the mouse. Front. Biosci. *11*, 313–327.

McGuire, S.E., Le, P.T., Osborn, A.J., Matsumoto, K., and Davis, R.L. (2003). Spatiotemporal rescue of memory dysfunction in Drosophila. Science *302*, 1765–1768.

Miesenbock, G., and Kevrekidis, I.G. (2005). Optical imaging and control of genetically designated neurons in functioning circuits. Annu. Rev. Neurosci. *28*, 533–563.

Moll, J.R., Ruvinov, S.B., Pastan, I., and Vinson, C. (2001). Designed heterodimerizing leucine zippers with a range of pIs and stabilities up to 10(-15) M. Protein Sci. *10*, 649–655.

Osterwalder, T., Yoon, K.S., White, B.H., and Keshishian, H. (2001). A conditional tissue-specific transgene expression system using inducible GAL4. Proc. Natl. Acad. Sci. USA *98*, 12596–12601.

Park, J.H., Schroeder, A.J., Helfrich-Forster, C., Jackson, F.R., and Ewer, J. (2003). Targeted ablation of CCAP neuropeptide-containing neurons of Drosophila causes specific defects in execution and circadian timing of ecdysis behavior. Development *130*, 2645–2656.

Resnitzky, D., Gossen, M., Bujard, H., and Reed, S.I. (1994). Acceleration of the G1/S phase transition by expression of cyclins D1 and E with an inducible system. Mol. Cell. Biol. *14*, 1669–1679.

Salvaterra, P.M., and Kitamoto, T. (2001). Drosophila cholinergic neurons and processes visualized with Gal4/UAS-GFP. Brain Res Gene Expr Patterns *1*, 73–82.

Stockinger, P., Kvitsiani, D., Rotkopf, S., Tirian, L., and Dickson, B.J. (2005). Neural circuitry that governs Drosophila male courtship behavior. Cell *121*, 795–807.

Suster, M.L., Seugnet, L., Bate, M., and Sokolowski, M.B. (2004). Refining GAL4-driven transgene expression in Drosophila with a GAL80 enhancer-trap. Genesis *39*, 240–245.

Ting, C.Y., Yonekura, S., Chung, P., Hsu, S.N., Robertson, H.M., Chiba, A., and Lee, C.H. (2005). Drosophila N-cadherin functions in the first stage of the two-stage layer-selection process of R7 photoreceptor afferents. Development *132*, 953–963.

Wang, Y., O'Malley, B.W., Jr., Tsai, S.Y., and O'Malley, B.W. (1994). A regulatory system for use in gene transfer. Proc. Natl. Acad. Sci. USA *91*, 8180–8184.

Wei, Q., Marchler, G., Edington, K., Karsch-Mizrachi, I., and Paterson, B.M. (2000). RNA interference demonstrates a role for nautilus in the myogenic conversion of Schneider cells by daughterless. Dev. Biol. *228*, 239–255.

White, B., Osterwalder, T., and Keshishian, H. (2001). Molecular genetic approaches to the targeted suppression of neuronal activity. Curr. Biol. *11*, R1041–R1053.

Wulff, P., and Wisden, W. (2005). Dissecting neural circuitry by combining genetics and pharmacology. Trends Neurosci. *28*, 44–50.

Yao, K.M., and White, K. (1994). Neural specificity of Elav expression—defining a Drosophila promoter for directing expression to the nervous-system. J. Neurochem. *63*, 41–51.